Jurnal Teknologi

Full Paper

OPTIMIZATION OF GOLD AND SILVER NANOPARTICLES PRODUCTION BY LASER ABLATION IN DEIONIZED WATER

Mohammed A. Al-Azawi, Noriah Bidin*, M. Abdullah, Khaldoon N. A. , Hayder J. Al-Asedy

*Advance Photonic Science Institute, Faculty of Science, Universiti Teknologi Malaysia, 81310, UTM Johor Bahru, Johor, Malaysia

Article history
Received
10 October 2014
Received in revised form
10 December 2014
Accepted
13 January 2015

*Corresponding author
noriah@utm.my

Graphical abstract

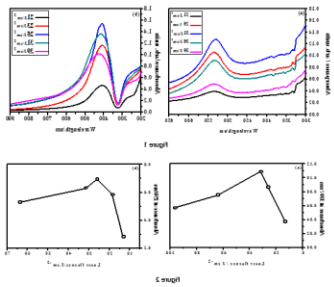

Abstract

Colloidal solutions of gold and silver nanoparticles (NPs) were synthesized using a Q-switched Nd:YAG laser (1064 nm, 6 ns, 1 Hz) ablation. Gold and silver bars were immersed in deionized water and irradiated by laser pulses for 4 min. The laser fluence was verified within the range of 21 – 39 J/cm^2 with a fixed beam diameter of 1.6 mm. The effect of laser pulse fluence on both size and ablation efficiency of gold and silver nanoparticles were studied. The optical spectral characterization and morphological analysis of these nanoparticles were carried out by UV-Vis spectrophotometer and transmission electron microscopy (TEM), respectively. The average particle size for Au and Ag are 38.0 ± 10.3 nm and 31.3 ± 10.5 nm at corresponding optimized laser fluence of 31 and 25 Jcm^{-2} respectively.

Keywords: Laser ablation, laser fluence, nanoparticles, gold and silver colloid

Abstrak

Penyelesaian koloid emas dan nanopartikel perak (NPS) telah disintesis menggunakan Nd Q-switched: YAG laser (1064 nm, 6 ns , 1 Hz) ablation . Bar emas dan perak telah direndam di dalam air ternyahion dan radiasi oleh denyutan laser untuk 4 min. The fluens laser telah disahkan dalam lingkungan 21-39 J/cm^2 dengan diameter rasuk tetap sebanyak 1.6 mm. Kesan laser nadi fluens di kedua-dua saiz dan ablasi kecekapan emas dan perak nanopartikel telah dikaji. Pencirian spektrum optik dan analisis morfologi nanopartikel ini telah dijalankan oleh UV-Vis spektrofotometer dan penghantaran elektron mikroskop (TEM), masing-masing . Saiz zarah purata bagi Au dan Ag adalah 38.0 ± 10,3 nm dan 31.3 ± 10,5 nm masing-masing pada dioptimumkan fluens laser pada 31 dan 25 Jcm^2 yang sepadan.

Kata kunci: Laser, Laser fluens, nanopartikel, emas dan perak koloid

1.0 INTRODUCTION

Over recent years, there has been an explosive growth of interest in the development of novel gel-phase materials based on small molecules [1]. It has been recognised that an effective gelator should possess functional groups that interact with each other via temporal associative forces. This process leads to the formation of supramolecular polymer-like structures [2] which then aggregate further, hence gelating the solvent. Supramolecular interactions between building blocks that enable gel formation include hydrogen bonds, interactions, solvatophobic effects and van der Waals forces [3]. Recently, great

emphasis has been placed on ways in which the structure of the gelator can control gel formation [4]. This has led to the investigation of a wide range of structurally diverse gelators, including those with dendritic structures [5]. Combinatorial libraries have also been investigated to enable the discovery of gelators with tunable properties [6].

In some cases, which are still relatively rare, two component gelators have been reported [7-9]. The two components interact with one another to form a complex, which is then capable of further supramolecular self-assembly leading to gelation. In 2001, we made a preliminary report of the first dendritic two component system for the gelation of organic solvents [10]. This two component system has a number of features which are important for effective gel formation: a) acid-base interactions between components, b) dendritic branching, c) aliphatic diamine spacer chain. This communication illustrates how using two components enhances the tunability of gel-phase materials, and indicates three ways in which macroscopic properties and microstructural features of the gel can be controlled.

As might be expected, the concentration of the gelator system controls the structure and properties of the gel. The solvated gelator network was observed using cryo transmission electron microscopy (cryo TEM) at different concentrations, maintaining a 2:1 (dendrimer:diamine) ratio. At low concentration, thin fibres were present, which at higher concentration aggregate and assemble into thick fibre bundles. The effect of molar concentration on the *thermally reversible gel-sol phase transition* (T_{gel}) was monitored using the tube inversion technique [11]. The validity of this approach, and the reversibility of the phase transition, was checked with differential scanning calorimetry. As the molar concentration of the dual components as shown in Table 1.

2.0 EXPERIMENTAL

Noble metals of gold and silver plates were employed for this research as target materials. Gold plate with higher than (99.999 %) purity, depth of 2 mm, and its diameter 20 mm. Silver plate with high purity of (99.998 %), thickness of 2 mm, and surface area of 25× 25 mm^2. Subsequently, plates were cleaned by ethanol and placed with ablation vessel in ultrasonically bath and rinsed with deionized water before each experiment to eliminate contaminants. The targets were kept at the bottom of a 2.5 cm × 2.5 cm–Pyrex vessel filled with ultrapure 18.2 MΩ deionized water as a layer thickness of a 1.8 mm above its surface. Pulsed Nd:YAG laser with fundamental (1064 nm) wavelength, pulse duration 6 ns and repetition rate of 1 Hz was employed for ablation as irradiation source. By using a lens with a focal length of 100 mm, the laser beam at a spot size of 1.6 mm in diameter with laser fluence of 21-39 J/cm^2 was focused onto the target surface. During ablation process, the Au and Ag colloidal solution was typically stirred by magnetic stirrer to remove the NPs produced from the laser path. Laser ablation process lasted for 4 minutes at room temperature, and the color of solution gradually changed to red and yellow with the increase of ablation time for gold and silver plate, respectively. It signified the presence of NPs.

The optical spectral characterization of the gold and silver colloidal solutions was measured with a UV-Vis spectrophotometer (Perkin-Elmer, Lambda 25). A 0.5 cm pathlength quartz cuvette was utilized for the absorption measurements. A transmission electron microscope (TEM), Philips CM12, operating at 120 kV accelerating voltage, was used to acquire micrographs of the resultant gold and silver nanoparticles. The gold and silver colloidal solutions were placed in the ultrasonic bath for 20 min. Subsequently, a small drop of sample solution was put on the carbon-coated copper grid, and dried at room temperature. More than hundred particles were computed to determine the size (diameter) and its distribution for each of the sample.

3.0 RESULTS AND DISCUSSION

Figure 1a and b presented typical UV-Vis optical spectra of colloidal solution produced by ablating Au and Ag targets in deionized water. The absorbance of gold and silver colloids demonstrated the characteristic features of the surface plasmon resonance SPR. The prominent band of SPR peak position of gold and silver observed at around 530-536 nm and 406-412 nm respectively, as a function of the laser fluence. The presence of prominent and consistent single peak indicated that the obtainable nanoparticles are nearly in spherical configuration and this is validated by the TEM examination. The morphology observation of the colloids will be discussed in the later part of this report. The absorption due to the interband transition is sensitive to the amount of particles and does not shift noticeable with the particle size [26, 28]. Thus, the absorption of the solution at the wavelengths of interband transitions can be employed as a measure of the total amount of gold particles in the solution, having nanoparticles of different sizes, clusters, and free gold atoms [29]. Therefore, the ablation efficiency was estimated from the absorbance of the interband transition for gold and silver at 330 nm and 250 nm, respectively.

The laser beam was adjusted at a spot size of 1.6 mm in diameter and focused using a lens 10 cm onto the gold surface. The different laser pulse fluences between 21-39 J/cm^2 were strike on the target for 4 minutes. On the basis of experimental data illustrated in Figure 1, there is a correlation between the ablation efficiency and the particle size of the colloids at certain laser fluence. The characteristics of both the absorption spectrum SPR peak and the interband transition are affected by the variation of

laser fluence. It is found that both SPR peak and interband transition are increased with laser fluence and the SPR peak position is realized slightly shifted toward shorter wavelength (blue shift).

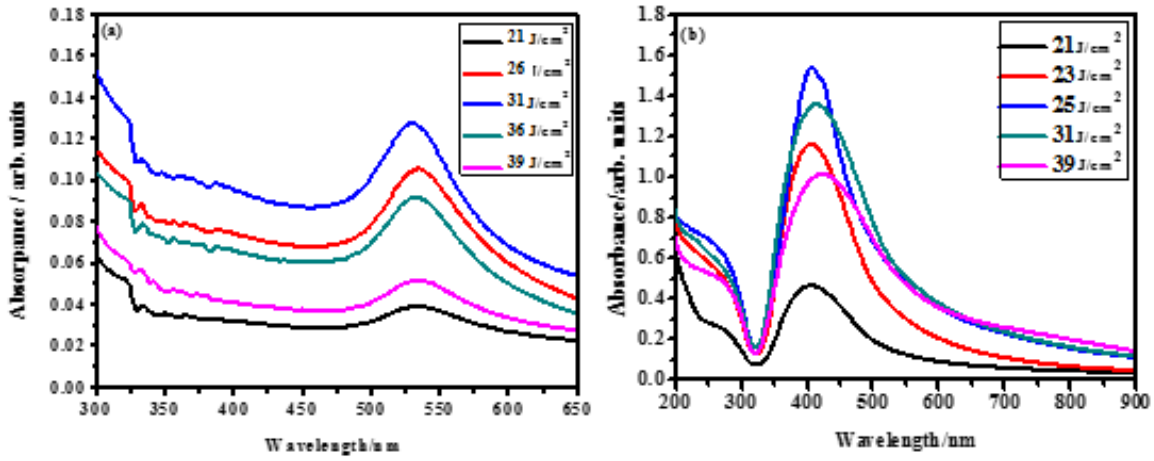

Figure 1 UV-Vis optical spectra of colloidal solution produced by ablating Au and Ag targets

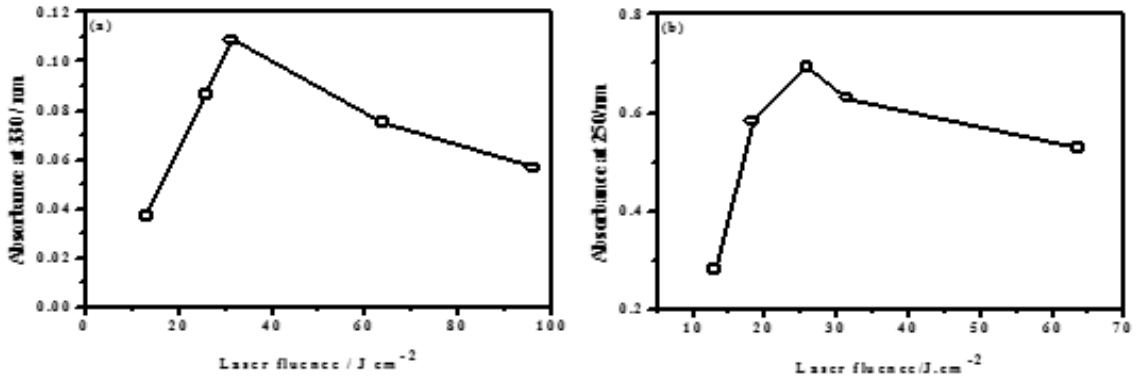

Figure 2 Laser fluency against absorbance

These results indicate that an increase in ablation efficiency and decrease in particle size with the increase of laser fluence. But all ablation efficiency increased and reached maximum value for gold and silver at laser fluence of 31 and 25 J/cm^2, respectively. Beyond these values, the ablation efficiency decreased significantly and the SPR peak position changed towards a longer wavelength. These values of laser fluence at the maximum ablation efficiency are considered as optimal condition for gold and silver nanoparticles as shown in Figure 2a and b. This can be understood by self-absorption process because the ablation of metals in the solution system leads to generate metal particles on the path of the incident laser light which can absorb the laser light [26]. The absorbed photon can thermally excite the lattice of metal particles and its temperature rises significantly so that the nanoparticle starts to fragment. The fragmentation rate of large particles must increase with increasing the laser fluence, which corresponds to the increased concentration of the nanoparticles in the solution namely the increase of the ablation efficiency and a smaller particle size distribution is also in agreement with blue shift. The increase of ablation efficiency may be due to the strong plasma pressure induced by the higher laser fluence, causing further ablation, material reaction with the liquid phase [29]. But at high laser fluence, the effect of the self-absorption may be quite significant because many metal particles are formed. Hence the self-absorption can reduce the intensity of incident laser to reach the target surface. In this case, the intensity of plasma plume decays and its effect on the target surface related the ablation effects decreased, consequently no further increase in the concentration of the nanoparticles [30]. Thereby, the ablation efficiently decreases and the SPR peak

position is shifted toward longer wavelength due to the aggregation of the particles and insensitivity to the laser fluence, hence the particle size increases. These results were validated by transmission electron microscopy TEM examination. Figure 3 and 4 show images of TEM of Au and Ag nanoparticles, respectively. Each frame is accompanied with the histograms of the particle size distribution. The results yielded by analysis of the particle size distribution for each case are summarized in Table 1.

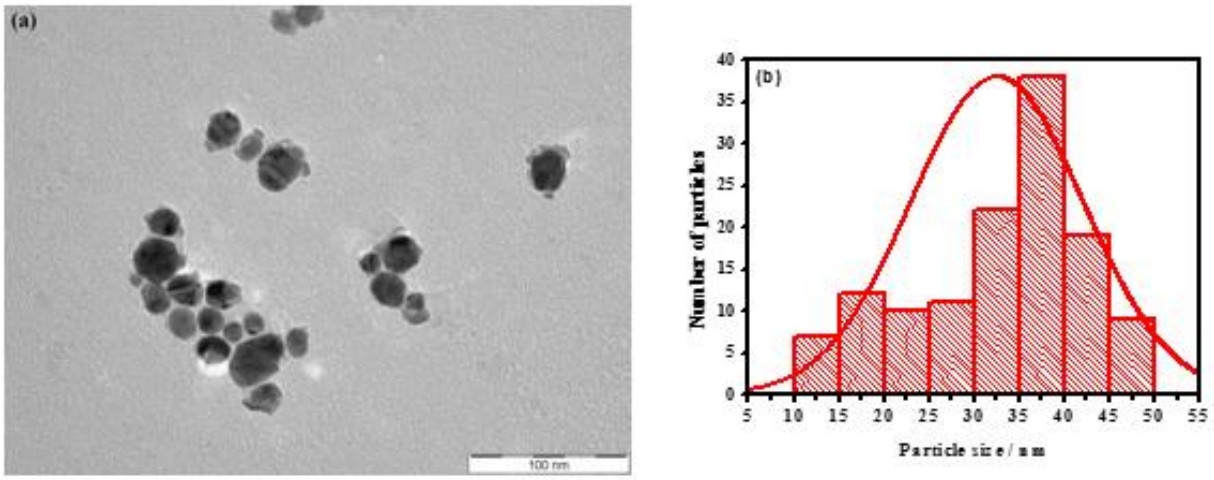

Figure 3 Transmission electron microscopy TEM examination of Au

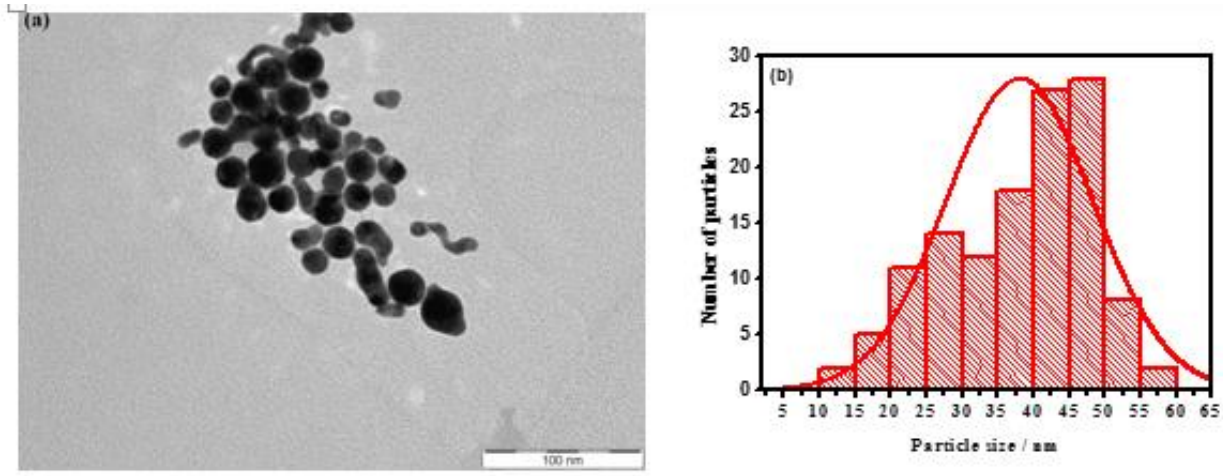

Figure 4 Transmission electron microscopy TEM examination of Ag

Table 1 Analysis of the particle size distribution

Metal	Laser fluence J/cm²	Average particle size (nm)	Standard deviation (nm)
Au	31	38.0	10.3
Ag	25	31.3	10.5

From TEM images for both Au and Ag, majority of the nanoparticles having spherical shape, relatively high aggregation and some chains of accreted particles. The corresponding histogram of its particle size distribution shows that the particle size distribution is more broadening with an average particle size of 38.0 and 31.3 nm for Au and Ag nanoparticles, respectively. As mentioned earlier, this is attributed from the used of high laser fluence and longer wavelengths. To tune average particle size and size distribution with less aggregation of nanoparticles, laser-induced fragmentation technique was employed. However, determination of optimum laser fluence plays an important role to raise the density of the ablated species.

In this work, ablation efficiency of Au and Ag nanoparticles are found increased continuously with laser fluence until the achievement of maximum value. Beyond that the ablation efficiency is decreased exponentially. This mean the size of nanoparticles is decreased by increasing the laser fluence. At low laser fluence, this finding is in a good agreement with Dorranian *et al*., [31] who used Ag ablation. They found that the amount and size of silver nanoparticles prepared by wavelength of 1064 nm at 7 ns pulse width increases with laser fluence. At high laser fluence after optimum value, the ablation efficiency and particle size are found inversely proportional with laser fluence. The later result is quite different may be due to the difference in laser fluence used for ablation.

4.0 CONCLUSION

Gold and silver nanoparticles were successfully synthesized by pulsed laser ablation in deionized water at different fluences of laser pulse. The effect of laser pulse fluence on both size and ablation efficiency of gold and silver nanoparticles were studied. The self – absorption of laser pulse in colloidal solutions caused a significant influence on the ablation efficiency and particle size. It is found that the ablation efficiency increases (whereby the particle size decreases) when laser fluence increases until its maximum value at laser fluence of of 31 and 25 J/cm2 for gold and silver, respectively; subsequently, the ablation efficiency rapidly decreased with increasing the laser fluence. TEM micrographs and UV-Vis spectrum indicate that the nanoparticles are revealed in spherical shape. The average particle size of gold and silver nanoparticles is 38.0 and 31.30 nm, respectively.

Acknowledgement

We like to express our thanks to the government of Malaysia through RUG-Flagship vote 00G79 for the financial support in this project.

References

[1] C. Liang, T. Sasaki, Y. Shimizu, and N. Koshizaki. 2004. Pulsed-laser Ablation of Mg in Liquids: Surfactant-directing Nanoparticle Assembly for Magnesium Hydroxide Nanostructures. *Chemical physics letters*. 389: 58-63.

[2] Y. Lu, M. Yu, M. Drechsler, and M. Ballauff. 2007. Ag Nanocomposite Particles: Preparation, Characterization and Application. *In Macromolecular symposia*. 97-102.

[3] C. P. Poole and F. J. Owens. 2003. *Introduction to Nanotechnology*. 19(5): 145-150.

[4] M. Raffi, F. Hussain, T. Bhatti, J. Akhter, A. Hameed, and M. Hasan. 2008. Antibacterial Characterization of Silver Nanoparticles Against E. Coli ATCC-15224. *Journal of Materials Science and Technology*. 24: 192-196.

[5] R. A. Sperling, P. R. Gil, F. Zhang, M. Zanella, and W. J. Parak. 2008. Biological Applications of Gold Nanoparticles. *Chemical Society Reviews*. 37: 1896-1908.

[6] P. K. Jain, I. H. El-Sayed, and M. A. El-Sayed. 2007. Au Nanoparticles Target Cancer. *Nano Today*. 2: 18-29.

[7] A. M. Schwartzberg, T. Y. Oshiro, J. Z. Zhang, T. Huser, and C. E. Talley. 2006. Improving Nanoprobes Using Surface-Enhanced Raman Scattering From 30-Nm Hollow Gold Particles. *Analytical chemistry*. 78: 4732-4736.

[8] V. Amendola and M. Meneghetti. 2009. Size Evaluation of Gold Nanoparticles Bby UV−Vis Spectroscopy. *The Journal of Physical Chemistry C*. 113: 4277-4285.

[9] D. Schaadt, B. Feng, and E. Yu. 2005. Enhanced Semiconductor Optical Absorption Via Surface Plasmon Excitation In Metal Nanoparticles. *Applied Physics Letters*. 86: 063106.

[10] K. Kneipp, M. Moskovits, and H. Kneipp. 2006. *Surface-Enhanced Raman Scattering: Physics and Applications*. 103: Springer.

[11] S. Pillai, K. Catchpole, T. Trupke, and M. Green. 2007. Surface Plasmon Enhanced Silicon Solar Cells. *Journal of Applied Physics*. 101: 093105.

[12] P. K. Jain, X. Huang, I. H. El-Sayed, and M. A. El-Sayed. 2008. Noble Metals on the Nanoscale: Optical and Photothermal Properties and Some Applications in Imaging, Sensing, Biology, and Medicine. *Accounts of Chemical Research*. 41: 1578-1586.

[13] M. Shao, L. Lu, H. Wang, S. Luo, and D. D. D. Ma. 2009 Microfabrication of a New Sensor Based on Silver and Silicon Nanomaterials, and Its Application to the Enrichment and Detection of Bovine Serum Albumin Via Surface-Enhanced Raman Scattering. *Microchimica Acta*. 164: 157-160.
[14] M. M. Maye, Y. Lou, and C.-J. Zhong. 2000. Core-shell Gold Nanoparticle Assembly as Novel Electrocatalyst of CO Oxidation. *Langmuir*. 16: 7520-7523.
[15] P. Sen, J. Ghosh, A. Abdullah, and P. Kumar. 2003. Preparation of Cu, Ag, Fe and Al Nanoparticles by the Exploding Wire Technique. *Journal of Chemical Sciences*. 115: 499-508.
[16] A. R. Siekkinen, J. M. McLellan, J. Chen, and Y. Xia. 2006. Rapid Synthesis of Small Silver Nanocubes by Mediating Polyol Reduction with a Trace Amount of Sodium Sulfide or Sodium Hydrosulfide. *Chemical Physics Letters*. 432: 491-496.
[17] S. Eustis and M. A. El-Sayed. 2006. Why Gold Nanoparticles Are More Precious Than Pretty Gold: Noble Metal Surface Plasmon Resonance and Its Enhancement of the Radiative and Nonradiative Properties of Nanocrystals of Different Shapes. *Chemical Society Reviews*. 35: 209-217.
[18] M. A. El-Sayed. 2001. Some Interesting Properties of Metals Confined in Time and Nanometer Space of Different Shapes. *Accounts of Chemical Research*. 34: 257-264.
[19] G. n. Schmid. 2010. *Nanoparticles from Theory to Application.* Weinheim: WILEY-VCH Verlag GmbH & Co. KGaA, Boschstr.
[20] J.-P. Sylvestre, A. V. Kabashin, E. Sacher, M. Meunier, and J. H. Luong. 2004. Stabilization and Size Control of Gold Nanoparticles During Laser Ablation in Aqueous Cyclodextrins. *Journal of the American Chemical Society*. 126: 7176-7177.
[21] A. Fojtik and A. Henglein. 1993. Laser Ablation of Films and Suspended Particles in a Solvent: Formation of Cluster and Colloid Solutions. *Berichte der Bunsen-Gesellschaft*. 97: 252-254.
[22] H. Imam, K. Elsayed, M. A. Ahmed, and R. Ramdan. 2012. Effect of Experimental Parameters on the Fabrication of Gold Nanoparticles via Laser Ablation. *Optics and Photonics Journal*. 2: 73.
[23] E. Carpene, D. Höche, and P. Schaaf. 2010. Fundamentals of Laser-Material Interactions. In Laser Processing of Materials, ed: Springer. 21-47.
[24] T. E. Itina. 2010. On Nanoparticle Formation by Laser Ablation in Liquids. *The Journal of Physical Chemistry C 2010*. 115: 5044-5048.
[25] N. V. Tarasenko and A. Butsen. 2010. Laser Synthesis and Modification of Composite Nanoparticles in Liquids. *Quantum Electronics*. 40: 986.
[26] T. Tsuji, K. Iryo, Y. Nishimura, and M. Tsuji. 2001. Preparation of Metal Colloids by a Laser Ablation Technique in Solution: Influence of Laser Wavelength on the Ablation Efficiency (II). *Journal of Photochemistry and Photobiology A: Chemistry*. 145: 201-207.
[27] K. A. Elsayed, H. Imam, M. Ahmed, and R. Ramadan. 2013. Effect of Focusing Conditions and Laser Parameters on the Fabrication of Gold Nanoparticles Via Laser Ablation in Liquid. *Optics & Laser Technology*. 45: 495-502.
[28] F. Hajiesmaeilbaigi, A. Mohammadalipour, J. Sabbaghzadeh, S. Hoseinkhani, and H. Fallah. 2006. Preparation of Silver Nanoparticles by Laser Ablation and Fragmentation in Pure Water. *Laser Physics Letters*. 3: 252.
[29] G. Yang. 2012. *Laser Ablation in Liquids: Principles and Applications in the Preparation of Nanomaterials*. CRC Press.
[30] J.-P. Sylvestre, S. Poulin, A. V. Kabashin, E. Sacher, M. Meunier, and J. H. Luong. 2004. Surface Chemistry of Gold Nanoparticles Produced by Laser Ablation in Aqueous Media. *The Journal of Physical Chemistry B*. 108: 16864-16869.
[31] D. Dorranian, S. Tajmir, and F. Khazanehfar. 2013. Effect of Laser Fluence on the Characteristics of Ag Nanoparticles Produced by Laser Ablation. *Soft Nanoscience Letters*. 3: 93.